

Performance of underwater data transmission using incoherent modulation MFSK in very shallow waters

Jan H. Schmidt, Aleksander M. Schmidt, Iwona Kochańska, Ryszard Studański, and Andrzej Żak

Abstract—Ensuring universal and stable underwater communication in shallow waters for various environmental conditions is a difficult scientific and engineering task. This applies in particular to underwater communication systems that use acoustic waves in very shallow underwater channels, where multipath propagation permanently occurs. The article provides assumptions for a system working with incoherent M -ary Frequency-Shift Keying (MFSK) modulation, along with guidelines for eliminating the impact of the multipath phenomenon. The results of experimental tests carried out in a lake for two seasons and, therefore, different sound velocity profiles are presented. For comparison purposes, three transducers placed at different depths, including at the bottom of the reservoir, were used to receive the transmitted signals.

Keywords—underwater acoustic communications; multipath propagation; MFSK; very shallow waters

I. INTRODUCTION

A very shallow water channel using acoustic waves is an extremely complex time-frequency varying channel. The implementation of an underwater communication system requires taking into account the unfavourable factors that characterise the underwater channel and examining their impact on the transmitted signal. This will allow the development of an underwater communication system that provides stable and reliable data transmission with a low error rate. The most important of these factors is multipath propagation, which causes the transmitted signal to be reflected from the bottom and the water surface and from objects in the water column. The receiver receives the signal arriving via the direct path and a significant number of signals arriving via paths obtained due to reflections. As a result, inter-symbol interference (ISI) occurs in the receiving path. Another factor is the Doppler effect, which is caused by the movement of the transmitter or receiver relative to each other. Its importance increases significantly if the transmission participants are in motion. In turn, the low propagation speed of the acoustic wave, the small bandwidth and the narrow band of the transducers used affect the data transmission rate [1], [2]. It should also be taken into account that the indicated parameters are variable and characterised by seasonal variability [3], [4].

Therefore, the underwater acoustic channel is considered one of the most difficult communication channels. This is

particularly true for the horizontal channel occurring in shallow and very shallow coastal waters with a high range-to-depth ratio, in which a strong multipath phenomenon permanently occurs, which makes the channel frequency selective. The implementation of data transmission in such a channel still poses major problems. They make it difficult to ensure high reliability and universality of the solution under variable channel conditions.

Existing and developing underwater acoustic communication systems make it possible to send data at high rate in vertical channels and much lower rate in horizontal channels. In order to implement data transmission, non-coherent and coherent modulations are traditionally used, with one or more carrier frequencies. Another group of such transmission systems use the most popular varieties of the spread spectrum technique, such as: chirp spread spectrum (CSS), direct sequence spread spectrum (DSSS), and frequency-hopping spread spectrum (FHSS) [5]-[8]. It is also worth mentioning the existence of efficient systems based on the orthogonal frequency division multiplexing (OFDM) technique [9], [10]. In order to improve the rate or quality of transmission, the multi-antenna (MIMO) technique is used [11].

Pilot signals in the form of sinusoidal signals at the edges of the data transmission system operating band have been used as preamble signals for the transmitted data frame for many years. In turn, in the shallow water channel, effective data frame synchronisation is achieved by using wideband signals in the preamble, mainly with linear frequency modulation (LFM) or with hyperbolic frequency modulation (HFM) [10], [12].

Commercial data transmission systems available on the market have rather limited transmission parameter configuration options. They provide the option to work in the presence of the Doppler effect with low values of the relative speed of the transmission participants, which are not acceptable in some applications. They are usually aimed at working in vertical underwater channels at high rates with the support of equalisers.

However, for a horizontal underwater channel where the multipath phenomenon occurs, they offer quite low transmission rate values [5].

The presented solution is dedicated to work in the configuration of a ship and an underwater object, which is

This work was supported by the National Centre for Research and Development under Project DOB-SZAFIR/01/B/017/04/2021.

Jan H. Schmidt, Aleksander M. Schmidt and Iwona Kochańska are with the Gdansk University of Technology, Faculty of Electronics, Telecommunications

and Informatics, Poland. (e-mail: {jan.schmidt, aleksander.schmidt, iwona.kochanska}@pg.edu.pl).

Ryszard Studański is with the Faculty of Electrical Engineering, Gdynia Maritime University, Poland (e-mail: r.studanski@we.umg.edu.pl).

A. Żak is with the Faculty of Mechanical and Electrical Engineering, Polish Naval Academy, Poland (e-mail: a.zak@amw.gdynia.pl).



placed on the bottom and is to provide robust transmission even in the case of being buried in bottom sediments. This entails the selection of an appropriate carrier frequency and transmission parameters that will effectively eliminate the impact of the multipath phenomenon and the Doppler effect. The requirement of robust, resistant and reliable transmission in very shallow waters was assumed, therefore MFSK modulation was used.

Experimental measurements were performed using several receiving hydrophones placed at different depths, including the bottom, to compare the performance of the receiver algorithms. The presented results were obtained for different seasons and, therefore, for different sound velocity profiles.

II. SYSTEM CONCEPT

The presented data transmission system was developed to implement communication between a ship and an underwater object, as shown in Fig. 1. A hydroacoustic antenna is submerged from the ship to the required depth, and the underwater object is located on the bottom and can be buried in the bottom sediments.

Each hydroacoustic signal sent by a transmitter using an underwater acoustic channel in which the multipath propagation phenomenon occurs reaches the receiver with many of its components shifted relative to each other in time. This channel can be presented as a linear filter whose complex low pass impulse response $h(\tau, t)$ is the sum of the impulse responses corresponding to all n propagation paths, in the form (1) [13], [14]. Each of these paths is described by the corresponding amplitude $a_n(t)$, phase $\varphi_n(t)$ and delay $\tau_n(t)$.

$$h(\tau, t) = \sum_{n=1}^{N(t)} a_n(t) e^{-j\varphi_n(t)} \delta(\tau - \tau_n(t)), \quad (1)$$

Delay τ applies only to paths obtained during reflections, and the value of these paths depends on their geometry. The number $N(t)$ is the maximum number of propagation paths during transmission, depending on t , and the individual components of the incoming signal are mutually uncorrelated.

The considered data transmission system transmits data based on a frame containing a preamble and data, as shown in Fig. 2.

The frame preamble consists of a pair of pulses of the same duration, which are based on the Hyperbolic Frequency Modulation (HFM) signal with an increasing (HFM-UP) and decreasing (HFM-DOWN) frequency during their duration. It is designed to detect the data frame, determine the beginning of

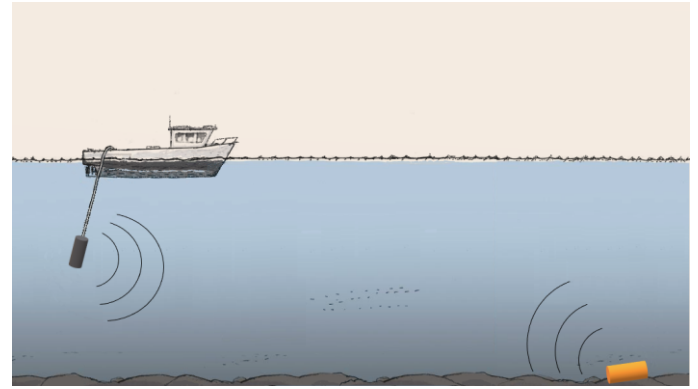


Fig. 1. Scheme of operation of the considered underwater communication system

the transmitted data and determine the Doppler shift [12]. Such a single pair of pulses as well as the combination of several such pairs of pulses have been tested by the authors, and are shown to have high reliability and accuracy in such waters, where signal fading occurs due to the multipath phenomenon. T_{PS} is the duration of the frame preamble pulse, T_S is the symbol duration, and T_{PG} is the unit guard interval for the frame preamble. The reliable functioning of this block has a significant impact on the accuracy of determining the occurrence of samples of consecutively received data symbols in the data frame.

Signals subjected to non-coherent modulation, in relation to coherent modulation, are characterised by better resistance in a channel with permanent multipath phenomena, because an energy detector is used in the receiver. The receiver for this modulation is based on an energy detector and is simple to implement and effective in operation. Moreover, it does not require the use of channel estimation methods and subsequent equalisation to obtain correct information about the carrier frequency phase in the case of such fading environments.

To effectively overcome the existing limitations of the shallow-water underwater acoustic channel, the M -ary Frequency-Shift Keying modulation was selected, which has been used for non-coherent communications for many years [13].

Spacecraft use FSK tones for communication in combination with non-coherent detection due to the very low receive signal power, severe signal distortion introduced by the channel, and high Doppler dynamics due to the significant relative motion between the transmitter and receiver [16], [17].

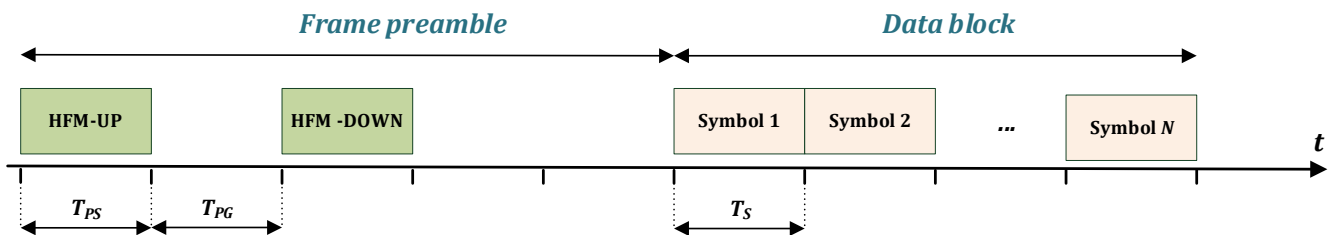


Fig. 2. Frame of transmitted data

For similar reasons, both the European Space Agency (ESA) and the National Aeronautics and Space Administration (NASA) are conducting research into the future use of orthogonal non-coherent MFSK for communications in deep space missions [18], [19]. For the effective use of this modulation in the shallow-water acoustic channel, appropriate parameters must also be selected.

MFSK modulation assumes the use of M distinct symbols. Traditional MFSK modulation uses only one tone from the available characteristic frequencies for each symbol. Hence, the modulation requires N orthogonal tones, where $N = M$, and each symbol can transmit $\log_2(M)$ bits. However, this causes an increase in the number of symbols M , which will require more bandwidth. Assuming data transmission using a single tone causes the transmitted signal to have a constant envelope, which is an obvious implementation advantage. The disadvantage of single-tone MFSK modulation is its low spectral efficiency, which for $M = N = 2$ is $n = 0.5$ bits/s/Hz, and for $M = N = 8$ is $n = 0.3750$ bits/s/Hz [13].

A. Multiple Frequency-Shift Keying (MFSK) modulation

The considered variant of traditional MFSK modulation was adapted to be immune to the multipath phenomenon and the influence of the Doppler effect.

1) Multipath phenomenon

In order to increase the immunity of transmitted signals to the multipath phenomenon for MFSK modulation, gaps must be used between successively transmitted symbols to avoid the influence of inter-symbol interference (ISI). This inter-symbol interference is caused by the extension of transmitted pulses and consequently causes the preceding pulses to overlap with the subsequent ones. These gaps are called guard intervals, guard times or guard periods and are marked as T_G . Their length should be at least equal to the maximum delay spread of the channel T_m , i.e. the condition $T_m \leq T_G$ must be met [20]-[23]. The maximum delay spread T_m is the time between the first and the last component of the received multipath signal, therefore the condition $T_m \ll T_S$ must be met simultaneously.

The transmitted low-pass FSK signal with characteristic frequency f_m and symbol duration T_S can be represented by the following formula (2) [13]:

$$s_m(t) = \sqrt{\frac{2E_s}{T_S}} \cos[2\pi f_m t + \varphi_m] , \quad (2)$$

$$(n-1)T_S \leq t \leq nT_S - T_G ,$$

$$1 \leq n \leq N , \quad 0 \leq m \leq M-1 ,$$

where E_s/T_S is the transmitted signal power, E_s is the energy per FSK symbol, f_m is the m -th characteristic frequency, φ_m is the unknown random phase associated with the m -th pulse, and N is the number of total symbols to be transmitted.

2) Doppler effect

Doppler shift is a result of the Doppler effect and to take its occurrence into account, the bandwidth reserved for the FSK

signal with a specific characteristic frequency f_m must be determined. The bandwidth is determined for the maximum permissible Doppler velocity v_{dmax} . Hence, the condition $B_D \ll B_S$ must be met, where B_D is the maximum Doppler spread and B_S is the bandwidth of the transmitted symbol signal [14].

The considered data transmission system operates using the carrier frequency $f_c = 15$ kHz, and the total operating bandwidth of the transducer is a maximum of $B_{FSK} = 5$ kHz. It was assumed that the maximum permissible Doppler velocity is equal to $v_{dmax} = 5$ m/s (~ 10 knots). This assumption leads to the following values of the maximum Doppler shift f_{dmax} at the edges of the operating band for the assumed value of the acoustic wave velocity in water $c = 1480$ m/s: for the left edge of the band $f_L = f_c - 2.5$ kHz = 12.5 kHz, the maximum Doppler shift is $f_{dmax} = 42.2$ Hz, and for the right edge of the band $f_R = f_c + 2.5$ kHz = 17.5 kHz, the maximum Doppler shift is $f_{dmax} = 59.1$ Hz. Therefore, the bandwidth for the FSK signal with a specific characteristic frequency f_m should be greater than about $2 \cdot 60$ Hz = 120 Hz.

However, to meet the orthogonality condition, a minimum separation between characteristic frequencies of $\Delta f = 1/T_S$ or its multiple should be used. In turn, so the Doppler effect does not affect the bands of adjacent characteristic frequencies, a minimum bandwidth for a single characteristic frequency of $B_S = \Delta f$ should be used, as presented in Fig. 3. Therefore, in the case of a transmission system based on 16FSK modulation, which uses pulses of length $T_S = 4$ ms, the bandwidth is $B_S = 250$ Hz. It is then required to use a bandwidth of $B_{FSK} = 16 \cdot \Delta f = 4000$ Hz.

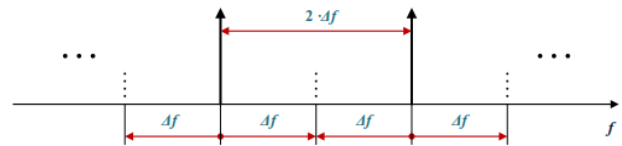


Fig. 3. Characteristic frequency separation scheme taking into account the influence of the Doppler effect

The operational diagram of the 16FSK data transmission system, including the use of guard intervals, is shown in Fig. 4.

3) Receiver implementation

The reception process is performed by a non-coherent receiver. Fig. 5 shows the block diagram of a receiver designed for MFSK modulation.

Its input receives a signal that has previously undergone analogue signal preprocessing, i.e. amplification and bandpass filtering, and is converted to a baseband signal. Signal samples are used to perform windowing operations, and then the signal is processed by calculating the discrete Fourier transform using the FFT algorithm. As a result of the transformation, a discrete signal spectrum is obtained, which is used to determine the power density spectrum of the discrete signal for subsequent symbols.

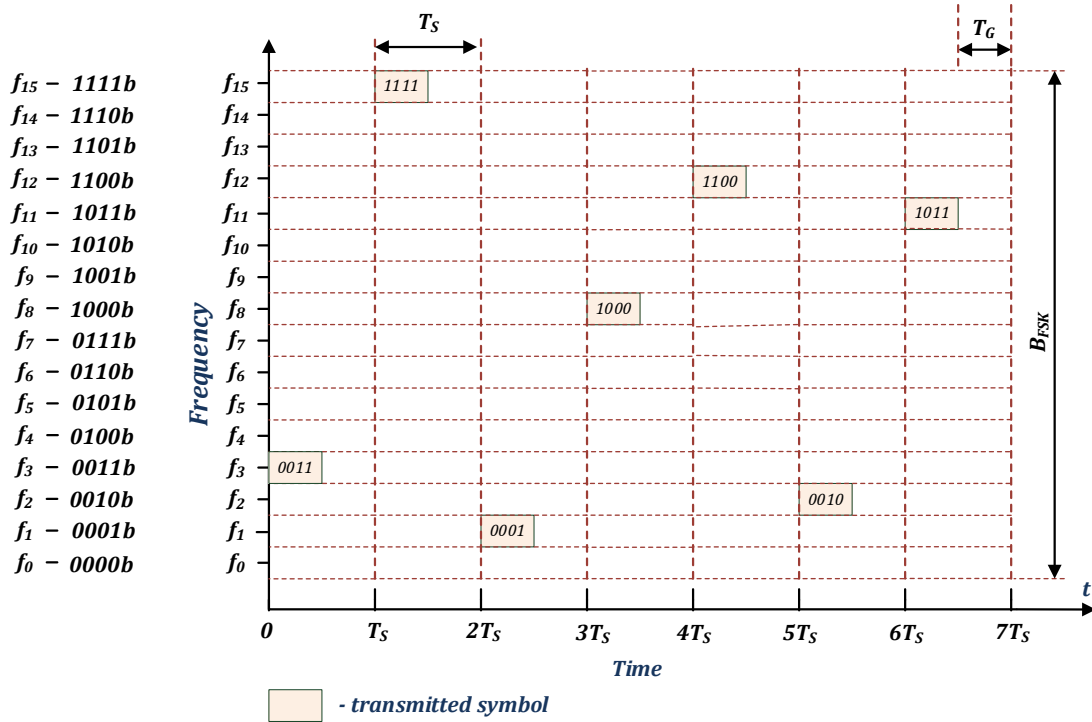


Fig. 4. Diagram of system with 16FSK and guard intervals between transmitted symbols.

The signal spectrum is obtained in the form of bands defined by Y_m values, and each of these bands represents a narrow band corresponding to the expected characteristic frequency f_m ($m = 0, \dots, M-1$). In the last step of the receiver operation, the decision system assigns the appropriate FSK symbol based on the criterion $f_m = \max(Y_m)$ while meeting an additional condition (3).

$$0.25 \cdot \max(Y_m) > Y_m \quad (3)$$

In the case of BFSK modulation, one comparison must be performed, and for 4FSK modulation, three comparisons, i.e. $M - 1$ comparisons.

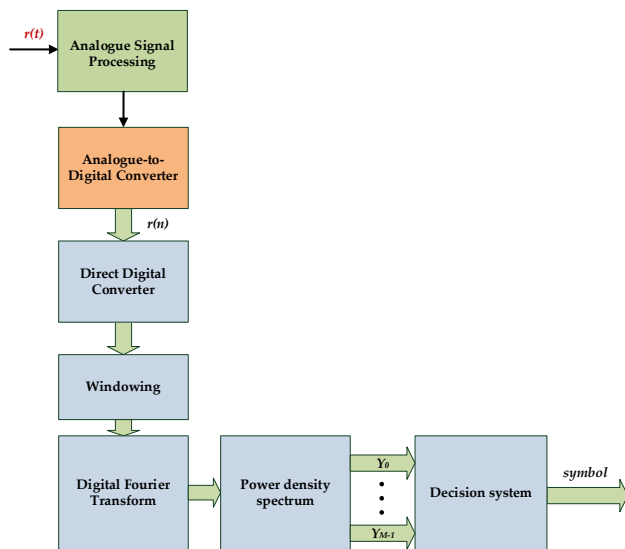


Fig. 5. The block diagram of the implemented MFSK receiver

This condition requires that the value of the maximum Y_m compared to each remaining expected Y_m is greater than 25% of its value. Failure to meet this condition results in information about a symbol reception error being generated.

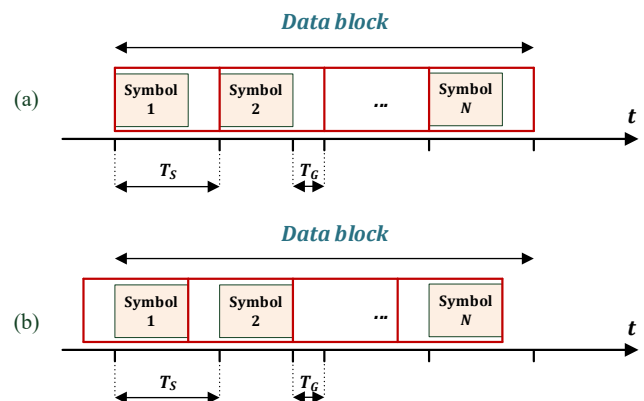


Fig. 6. Analysis window in the frame of transmitted symbols for extreme permissible window shifts λ , a) perfectly synchronised analysis window $\lambda = 0$, b) analysis window with analysis window shift $\lambda = -T_G$

The indirect advantage of using the guard interval T_G after the symbol signal is transmitted is that the data frame synchronisation system in both the MFSK and MC-MFSK modulation techniques can result in significantly inaccurate synchronisation. This is shown in Fig. 6, where two extreme cases of the analysis window shift are shown. The analysis window includes the duration of a single symbol, which is the sum of the effective transmission time of the symbol signal ($T_S - T_G$) and the T_G gap time. The maximum permissible analysis window shift is equal to $\lambda = -T_G$. Hence, the permissible synchronisation error takes large values and is a mild criterion

of synchronisation accuracy for the correct functioning of the symbol receiver.

An effective method of increasing the spectral efficiency is to use multi-tone MFSK modulation. It uses several frequencies at once during symbol transmission instead of one frequency, as in the case of single-tone MFSK [24], [25]. This modulation method is analogous to multi-tone On Off Keying (OOK), and similarly to multi-tone MFSK, has a significant disadvantage, which consists in the difficulty of setting the threshold for correct symbol decision operation due to large amplitude fluctuations of the received signal. Both methods require a signal with a higher SNR compared to traditional MFSK modulation.

Another disadvantage of this modulation method is the lack of a constant number of expected tones in the reception process. This increases the uncertainty of the method's operation, which is especially undesirable for a channel with fading.

B. Multi-carrier Multiple Frequency-Shift Keying (MC-MFSK) modulation

Another effective technique that eliminates the major disadvantages of multi-tone MFSK modulation is to divide the available operating bandwidth into multiple subbands using single-tone MFSK modulation in parallel.

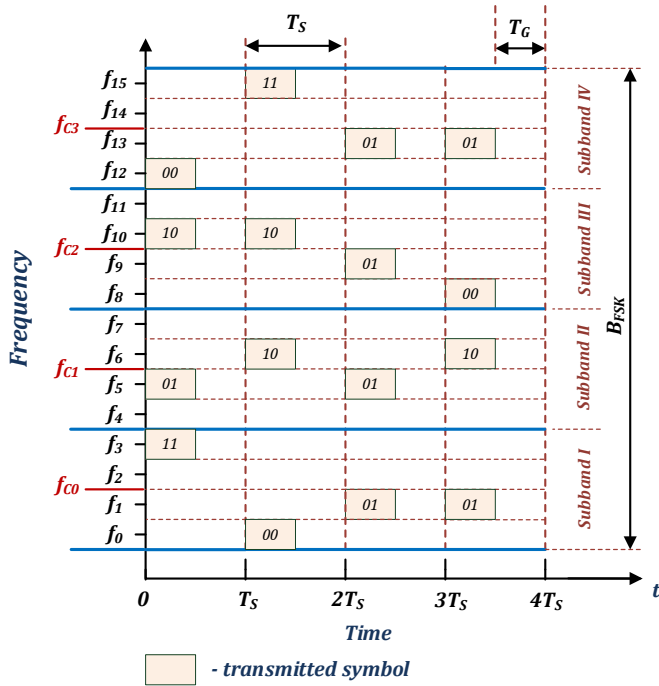


Fig. 7. Diagram of system with MC-4-FSK and guard interval between transmitted symbols

This technique provides higher transmission rates than single-tone MFSK modulation and uniqueness of signal reception in the subband compared to the multi-tone MFSK modulation method due to the elimination of the basic detection criterion which is the threshold for the operation of the symbol decision system. For each of the subbands, a decision system is used which determines the symbol for each of them separately. For each transmitted symbol in the subband, we expect only one tone to assign a symbol from the available set of M symbols. This technique using 4FSK modulation is shown in Fig. 7.

This figure shows a technique using 4FSK modulation in four subbands. In Subband I, pairs of bits 11 00 01 01 are transmitted successively, with the help of four successively transmitted symbols. In the BFSK band, which corresponds to the band allocated for 16FSK modulation, twice as much data is transmitted compared to this 16FSK modulation.

This technique uses the same methods of taking into account multipath phenomena and the Doppler effect as for the previously described MFSK modulation. Furthermore, during difficult conditions in the underwater channel, it is possible to transmit the same symbol over several sub-bands and to repeat the same symbols multiple times.

Figure 8 shows the envelope of signals for 4FSK modulation and the MC-4-FSK technique. In this modulation, bits 11 are transmitted using the characteristic frequency f_3 . In turn, for the MC-4-FSK technique, pairs of bits 00 00 11 11 were transmitted successively using the characteristic frequencies f_0, f_4, f_{11} and f_{15} . The comparison shows the need to use a linear amplifier for the MC-MFSK technique.

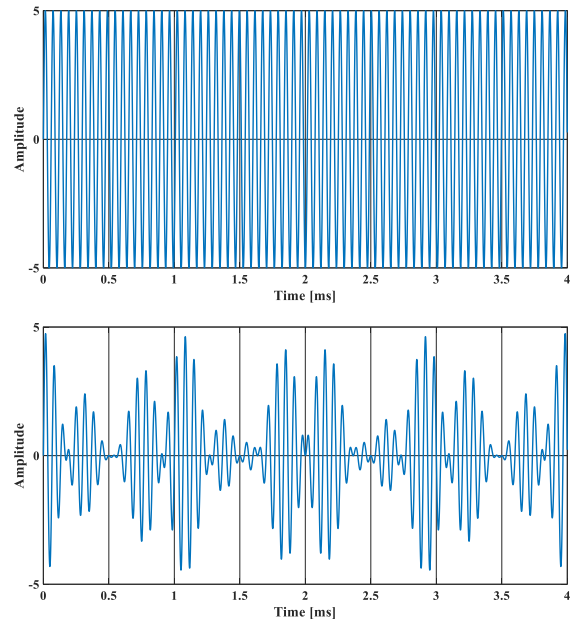


Fig. 8. Transmitted signals a) MFSK (f_3) b) MC-4-FSK (f_0, f_4, f_{11}, f_{15})

III. EXPERIMENTAL TESTS

To determine the robustness of the presented two modulation techniques for the underwater acoustic communication system operating in very shallow waters, a series of experimental tests were performed. The tests were conducted during several measurement sessions at the Hydroacoustic Research Station of the Gdańsk University of Technology on Lake Wdzydze, Poland for different seasons and consequently for different sound velocity distribution profiles.

On the transmitting side of the measurement system, signal samples were generated in the MATLAB computing environment on laptop computers and then converted to analogue form using an NI-USB 6363 from National Instruments. The signals prepared in this way were transmitted via a HTL-10 underwater telephone, whose basic task is to implement underwater communication with parameters

specified in the STANAG 1074 standard. In addition, as it is a Software-Defined Modems device, it is capable of working with any waveforms in the band from 1 kHz to 60 kHz.

Three hydrophones were used on the receiving side, connected to a B2008 multi-channel hydrophone amplifier from Etec ApS (Denmark). The amplified signals were converted from analogue to digital using an NI-USB 6356 from National Instruments, with a sampling rate of 200 kHz. The transmitting part of the system was located on a motorboat, and the receiving part of the system was placed on a floating container moored at the quay.

During the tests, signals were transmitted in the $B_{FSK} = 5$ kHz band and for the carrier frequency $f_c = 15$ kHz (12.5–17.5 kHz). The carrier frequency was set to achieve reception of the transmitted signals by a hydrophone buried in the bottom sediments. The selection was made based on papers related to the propagation of acoustic waves in bottom sediments, which have been published for 60 years [26]–[30]. The papers concern the results of measurements of the attenuation coefficients and the velocity of acoustic waves in various types of bottom sediments and the theoretical analysis of the propagation conditions in bottom sediments.

A. Autumn measurement session

The transmitting transducer was immersed to a depth of 5 m, and the depth of the water at the boat mooring points was approx. 10 m. The hydrophones were placed in a location where the lake depth was 4 m. The first one was placed on the bottom (depth of approx. 4 metres) and was buried in the bottom sediments. The second one was immersed to a depth of 3 m, and the third to a depth of 2 m.

Before taking the series of measurements, the sound velocity profile was measured. The results are presented in Fig. 9.

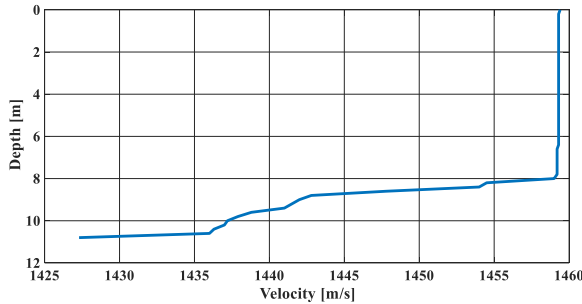


Fig. 9. Sound velocity profile in Lake Wdzydze measured in the autumn session

Hence, for this profile, the acoustic wave propagation paths determined for the transmitter placed at a depth of 5 metres provide a maximum range of about 600 m. Figure 10 shows the impulse responses with normalised amplitude obtained for each of the hydrophones, with a distance between the measurement stations of 250 m, and Fig. 11 for a distance of 500 m.

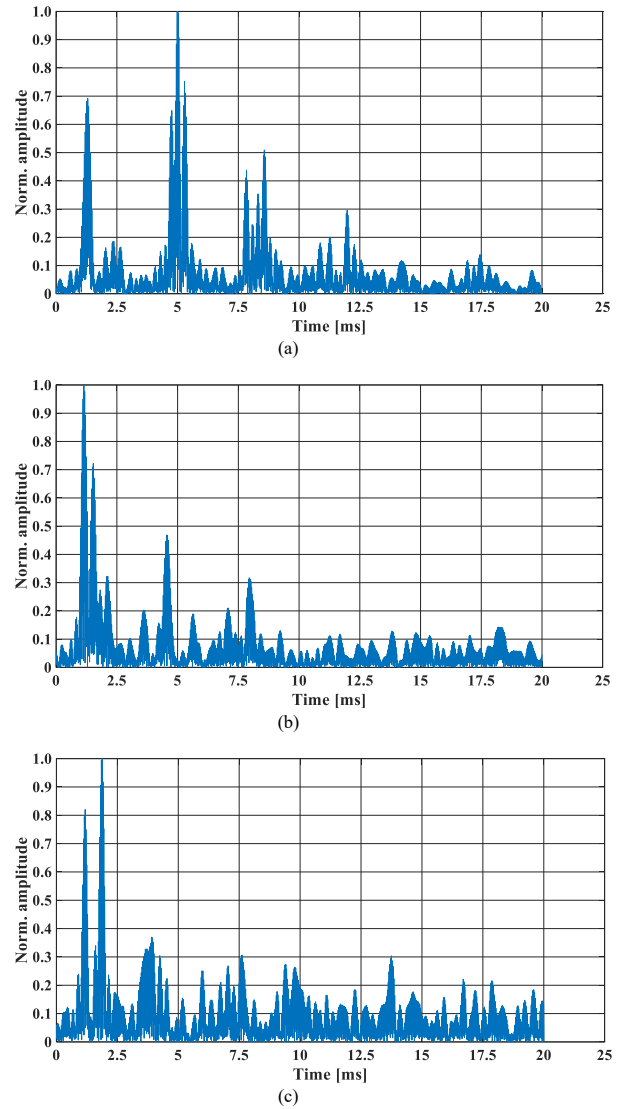


Fig. 10. Impulse response of the shallow-water channel for a transmitter-receiver distance of 250 m (a) hydrophone at the bottom (depth $h = 4$) (b) hydrophone at depth $h = 3$ (c) hydrophone at depth $h = 2$

Based on the obtained impulse response, the maximum delay spread of the channel T_m was determined for each of the hydrophones at a threshold of 0.2. For the distance between the measuring stations of 250 m, the following T_m values were obtained: (a) $T_m = 11$ ms – hydrophone at the bottom (depth $h = 4$); (b) $T_m = 7$ ms – hydrophone at depth $h = 3$; (c) $T_m = 17$ ms – hydrophone at depth $h = 2$. In turn, for the distance of 500 m, the following T_m values were obtained: (a) $T_m = 17$ ms – hydrophone at the bottom (depth $h = 4$); (b) $T_m = 16$ ms – hydrophone at depth $h = 3$; (c) $T_m = 33$ ms – hydrophone at depth $h = 2$.

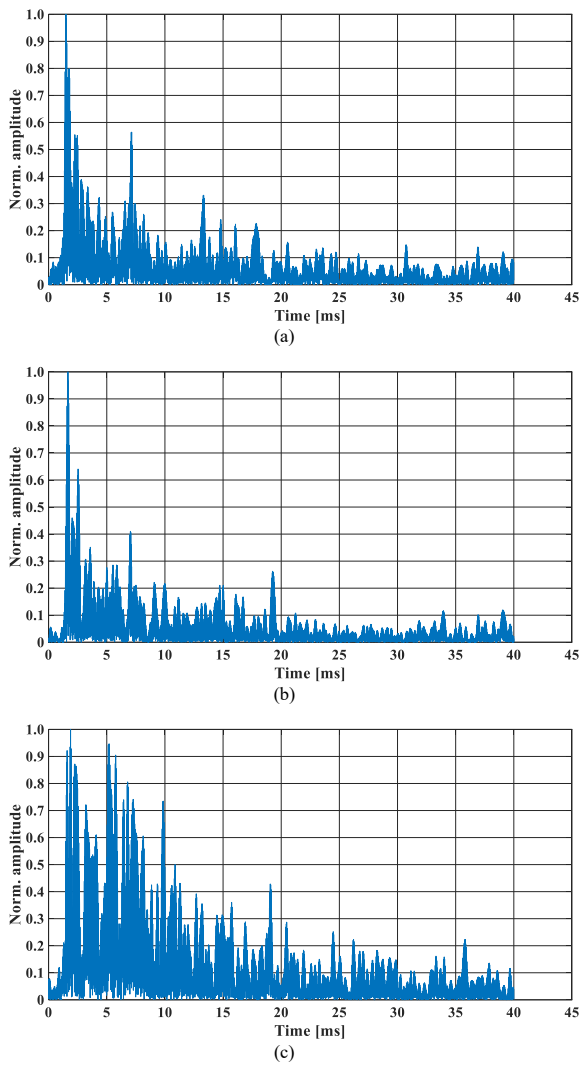


Fig. 11. Impulse response of the shallow-water channel for transmitter-receiver distance 500 m (a) hydrophone at the bottom (depth $h = 4$) (b) hydrophone at depth $h = 3$ (c) hydrophone at depth $h = 2$

Table I lists the determined bit error rates (BER) obtained for the distance between measurement stations of 250 m ($T_S = 64$ ms, $T_G = 64$ ms, SNR = 10 dB).

TABLE I
BIT ERROR RATES FOR 250 M

Modulation	Hydrophone depth [m]	T_m [ms]	BER
BFSK	4 (bottom)	11	0.001
	3	7	<0.001
	2	17	0.006
16FSK	4 (bottom)	11	0.009
	3	7	0.006
	2	17	0.009
MC-8-BFSK	4 (bottom)	11	0.004
	3	7	0.003
	2	17	0.011
MC-4-4FSK	4 (bottom)	11	0.008
	3	7	0.005
	2	17	0.013

Table II contains the bit error rates (BER) determined for the distance between measurement stations of 500 m ($T_S = 64$ ms, $T_G = 64$ ms, SNR = 10 dB).

TABLE II
BIT ERROR RATES FOR 500 M

Modulation	Hydrophone depth [m]	T_m [ms]	BER
BFSK	4 (bottom)	17	<0.001
	3	16	0.016
	2	33	0.002
16FSK	4 (bottom)	17	0.003
	3	16	0.001
	2	33	0.005
MC-8-BFSK	4 (bottom)	17	0.005
	3	16	0.003
	2	33	0.011
MC-4-4FSK	4 (bottom)	17	0.007
	3	16	0.004
	2	33	0.028

The results obtained for both distances between the measurement stations indicate that the signals with the centre frequency $f_c = 15$ kHz and the band $B_{FSK} = 5$ kHz reach the hydrophone placed at the bottom and the one buried in the bottom sediments (depth $h = 4$). For this hydrophone, the received impulse responses contain a similar character of multipath components for both distances. This is confirmed by the obtained values of the error rate for these channels. The greatest deterioration of the reception quality occurs for the hydrophone closest to the water surface.

B. Summer measurement session

In this measurement session, the lake depth at the boat moorings was about 8 m and the transmitting transducer was submerged to a depth of 4 m. On the receiving side, the lake depth was 6 m. On the receiving side, the first hydrophone was placed at the bottom (approx. 6 m depth) and buried in the bottom sediments. The second was immersed at a depth of 4 m, and the third at a depth of 2 m.

The measured sound velocity profile is presented in Fig. 12. The acoustic wave propagation paths determined on its basis for the transmitting transducer placed at a depth of 4 metres predicted a maximum range of 120 m.

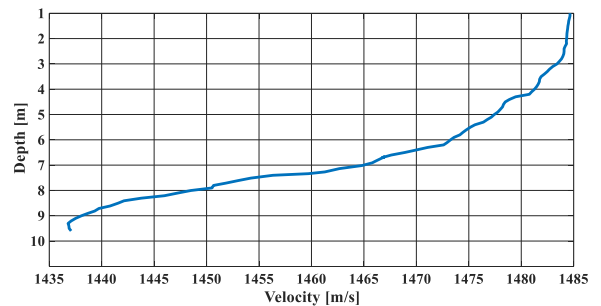


Fig. 12. Sound velocity profile in Lake Wdzydze measured in the summer session

Figure 13 shows the impulse responses obtained for each of the hydrophones at a distance of 100 m.

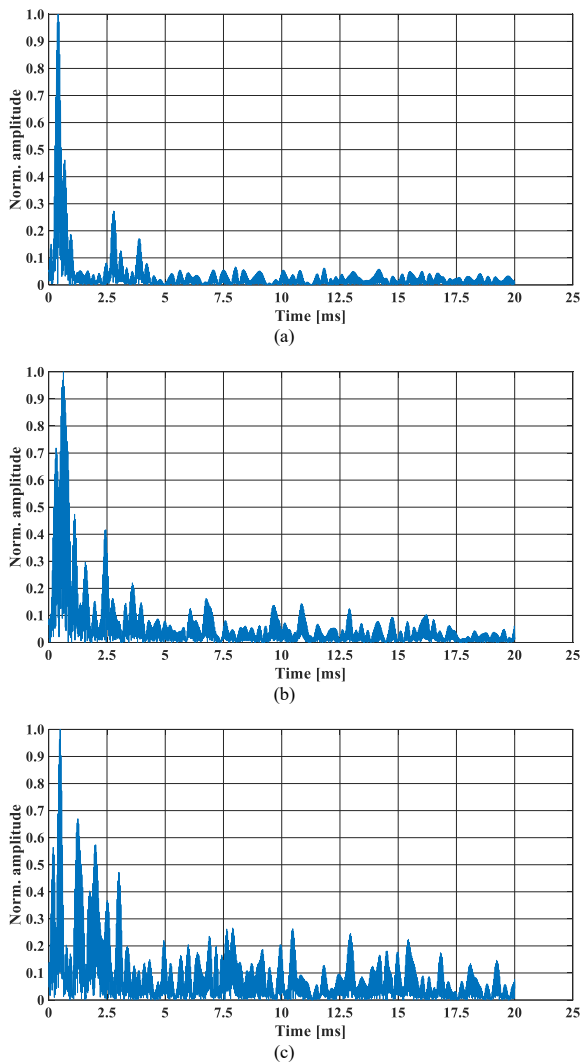


Fig. 13. Impulse response of the shallow-water channel for transmitter-receiver distance 100 m (a) hydrophone at the bottom (depth $h = 6$) (b) hydrophone at depth $h = 4$ (c) hydrophone at depth $h = 2$.

For this distance, the following T_m values were determined at a threshold of 0.2: (a) $T_m = 3$ ms – hydrophone at the bottom (depth $h = 6$); (b) $T_m = 4$ ms – hydrophone at depth $h = 4$; (c) $T_m = 16$ ms – hydrophone at depth $h = 2$.

TABLE III
BIT ERROR RATE FOR 100 M

Modulation	Hydrophone depth [m]	T_m [ms]	BER
BFSK	6 (bottom)	3	0.002
	4	4	0.003
	2	16	0.012
16FSK	6 (bottom)	3	0.004
	4	4	0.009
	2	16	0.015
MC-8-BFSK	6 (bottom)	3	0.003
	4	4	0.005
	2	16	0.022
MC-4-4FSK	6 (bottom)	3	0.008
	4	4	0.006
	2	16	0.019

Table III presents the bit error rates obtained for a distance between measurement stations of 100 m ($T_S = 64$ ms, $T_G = 64$ ms, SNR = 10 dB).

It follows from them that the results of the reception quality determined for the distance between measuring stations of 100 m are consistent with the results that were obtained for the distances of 250 m and 500 m. The best BER results are for the hydrophone placed on the bottom and buried in the bottom sediments, while with decreasing depth, the value of the reception quality deteriorates. The obtained results lead to the conclusion that MFSK modulation provides better reception quality in relation to the MC-MFSK technique for the same SNR value.

Based on the measured sound velocity profiles, the predicted acoustic wave propagation ranges for both seasons were determined. For the autumn, higher ranges were obtained compared to the summer. They were confirmed by the results of experimental measurements. For both MFSK modulation and the MC-MFSK technique, the BER values are lower for the summer, because the maximum delay spread value of the channel T_m and the nature of the multipath components in the channel impulse response have a decisive influence here.

CONCLUSION

Providing data transmission in shallow waters is a demanding task. One key aspect of implementing robust transmission is the method of taking into account the most unfavourable factors occurring in the underwater channel. The presented research results concern the considered data transmission system operating in the configuration of a ship and an underwater object, where the underwater object is placed on the bottom and can be buried in the bottom sediments. Experimental studies were conducted during two different seasons in the lake and made it possible to compare the underwater channel parameters obtained on the basis of measured channel impulse responses. The results were used in the evaluation of the functioning of the receiving algorithms for the two selected modulation techniques considered. The test results, presented in the form of graphs and tables, and especially the BER values, prescribe these techniques for operation in such a difficult underwater channel with strong multipath propagation.

The target data transmission system assumes the use of the modulation techniques indicated here using channel coding capable of eliminating single erroneous symbols.

ACKNOWLEDGEMENTS

The research presented in the article was carried out as part of the project ‘Underwater wireless communication system for unmanned and autonomous offshore platforms’. The program No. DOB-SZAFIR/01/B/017/04/2021 is financed by The National Centre for Research and Development.

The authors would like to thank their colleagues Michał Dolot and Stefan Szulc for their help in carrying out measurements.

REFERENCES

- [1] X. Lurton, “An Introduction to Underwater Acoustics: Principles and Applications,” Springer, 2010.
- [2] J. Hui, X. Sheng, “Underwater Acoustic Channel,” Springer, 2023.

- [3] Z. Klusek, A. Lisimenka, "Seasonal and diel variability of the underwater noise in the Baltic Sea," *The Journal of the Acoustical Society of America*, 139, pp. 1537–1547, 2016. <https://doi.org/10.1121/1.4944875>
- [4] B. Katsnelson, V. Petnikov, J. Lynch, "Fundamentals of Shallow Water Acoustics," Springer, 2012.
- [5] H. S. Dol, P. Casari, T. van der Zwan, R. Otnes, "Software-Defined Underwater Acoustic Modems: Historical Review and the NILUS Approach," *IEEE Journal of Oceanic Engineering*, vol. 42, pp. 722–737, 2017. <https://doi.org/10.1109/JOE.2016.2598412>
- [6] J.H. Schmidt, A.M. Schmidt, "Underwater Acoustic Communication System Using Broadband Signal with Hyperbolically Modulated Frequency," *Vibrations in Physical Systems*, 32(1):2021116, 2021. <https://doi.org/10.21008/j.0860-6897.2021.1.16>
- [7] J. Schmidt, I. Kochańska, A. Schmidt, "Performance of the Direct Sequence Spread Spectrum Underwater Acoustic Communication System with Differential Detection in Strong Multipath Propagation Conditions," *Archives of Acoustics*, 49, 2024. <https://doi.org/10.24425/aoa.2024.-148771>
- [8] J.H. Schmidt, "Using Fast Frequency Hopping Technique to Improve Reliability of Underwater Communication System," *Applied Sciences*, 10, no. 3: 1172, 2020. <https://doi.org/10.3390/app10031172>
- [9] I. Kochańska, J.H. Schmidt, J. Marszał, "Shallow Water Experiment of OFDM Underwater Acoustic Communications," *Archives of Acoustics*, 45(1), pp. 11–18, 2020. <https://doi.org/10.24425/aoa.2019.129737>
- [10] S. Zhou, Z. Wang, "OFDM for Underwater Acoustic Communications," John Wiley & Sons Ltd.: Chichester, UK, 2014.
- [11] J. H. Schmidt, A. M. Schmidt and I. Kochańska, "Multiple-Input Multiple-Output Technique for Underwater Acoustic Communication System," 2018 Joint Conference - Acoustics, Ustka, Poland, pp. 1–4, 2018. <https://doi.org/10.1109/ACOUSTICS.2018.8502439>
- [12] J. H. Schmidt, A. M. Schmidt, "Wake-Up Receiver for Underwater Acoustic Communication Using in Shallow Water," *Sensors*, no. 4: 2088, 2023. <https://doi.org/10.3390/s23042088>
- [13] J.G. Proakis, "Digital Communication," McGrawHill, NY, USA, 2000.
- [14] A.F. Molisch, "Wireless Communications," Wiley-IEEE Press: Amsterdam, The Netherlands, 2010.
- [15] D. Bayley, J. D. Ralphs, "Piccolo 32-tone telegraph system in diplomatic communication," *Proc IEE*, vol. 119, no. 9, pp. 1229–1236, 1972.
- [16] M. Baldi, F. Chiaraluce, N. Maturo, G. Ricciutelli, R. Abelló, J. De Vicente, M. Mercolino, A. Ardito, F. Barbaglio, S. Finocchiaro, "Coding for space telemetry and telecommand transmissions in presence of solar scintillation," in *Proc. Int. Workshop Tracking, Telemetry Command Syst. Space Appl. (TTC)*, pp. 1–8, Sep. 2016.
- [17] M. Baldi, F. Chiaraluce, N. Maturo, G. Ricciutelli, A. Ardito, F. Barbaglio, "Coded transmissions for space links affected by solar scintillation: Baseband analysis," *Int. J. Satell. Commun. Netw.*, vol. 37, no. 6, pp. 571–587, 2019. <https://doi.org/10.1002/sat.1299>
- [18] E. Satorius, P. Estabrook, J. Wilson, D. Fort, "Direct-to-Earth communications and signal processing for Mars exploration Rover entry, descent, and landing," *Interplanetary Netw. Prog. Rep.*, pp. 42–153, May 2003. [Online]. Available: <https://ipnpr.jpl.nasa.gov/>
- [19] ECOMTEC (Executive Summary Report), document ESA Study. ESA Contract Number 4000113507/15/N/FE, TAS-I, Callisto and ZELINDA, ECOMTEC Study, Nov. 2017.
- [20] I. Kochanska, Jan H. Schmidt, Aleksander M. Schmidt, "Study of probe signal bandwidth influence on estimation of coherence bandwidth for underwater acoustic communication channel," *Applied Acoustics*, Volume 183, 2021. <https://doi.org/10.1016/j.apacoust.2021.108331>
- [21] I. Kochańska, J. Schmidt, "Estimation of Coherence Bandwidth for Underwater Acoustic Communication Channel," 2018 Joint Conference - Acoustics, 1–9, 2018. <https://doi.org/10.1109/acoustics.2018.8502331>
- [22] R. Studański, A. Żak, "Results of impulse response measurements in real conditions," *Journal of Marine Engineering & Technology*, Volume 16, pp. 337–343, 2017. <https://doi.org/10.1080/20464177.2017.1378151>
- [23] A. Czapiewska, A. Luksza, R. Studanski, A. Żak, "Reduction of the Multipath Propagation Effect in a Hydroacoustic Channel Using Filtration in Cepstrum," *Sensors*, 20, 751, 2020. <https://doi.org/10.3390/s20030751>
- [24] K. Zachariasz, J. Schmidt, R. Salamon, "Code signals transmission using MFSK modulation in shallow waters," *Hydroacoustics*, Vol.4, pp. 261–264, 2001.
- [25] J. Schmidt, K. Zachariasz, R. Salamon, "Underwater communication system for shallow water using modified MFSK modulation," *Hydroacoustics*, Vol. 8, pp. 179–184, 2005.
- [26] A. B. Wood, D. E. Weston, "The propagation of sound in mud," *Acta Acustica united with Acustica*, pp. 156–162, 1964.
- [27] R.D. Stoll, G.M. Bryan, "Wave Attenuation in Saturated Sediments," *Journal of the Acoustical Society of America*, Vol. 47, pp. 1440–1447, 1970. <https://doi.org/10.1121/1.1912054>
- [28] R.D. Stoll, "Theoretical aspects of sound transmission in sediments," *Journal of the Acoustical Society of America*, Vol. 68(5), pp. 1341–1350, 1980. <https://doi.org/10.1121/1.385101>
- [29] R.D. Stoll, "Marine sediment acoustics," *Journal of the Acous. Society of America*, Vol. 77(5): 1789–1799, 1985. <https://doi.org/10.1121/1.391928>
- [30] M.S. Ballard, K.M. Lee, "The acoustics of marine sediments," *Acoustics Today*, Vol. 13(3), pp. 11–18, 2017.